DOI 10.1007/s11141-021-10068-w
Radiophysics and Quantum Electronics, Vol. 63, Nos. 5–6, October–November, 2020
(Russian Original Vol. 63, Nos. 5–6, May–June, 2020)

DEVELOPMENT OF PHOTOINJECTOR ACCELERATOR COMPLEX AT THE INSTITUTE OF APPLIED PHYSICS OF THE RUSSIAN ACADEMY OF SCIENCES: RESEARCH STATUS AND PROSPECTS

A. A. Vikharev,* A. L. Vikharev, E. I. Gacheva, O. A. Ivanov, S. V. Kuzikov, D. S. Makarov, M. A. Mart'yanov, S. Yu. Mironov, N. Yu. Peskov, A. K. Potemkin, M. Yu. Tret'yakov, and A. P. Shkaev

UDC 621.385

This work is devoted to the studies performed at the Institute of Applied Physics of the Russian Academy of Sciences and aimed at the development of the photoinjector accelerator complex, which ensures formation of the electron bunches with charges of up to 100 pC and particle energies of 3 to 5 MeV. The key elements of the complex are described, namely, the accelerating cavity powered by the klystron with an operation frequency of 2.45 GHz and a power of 5 MW, a photocathode based on diamond films, a high-power ultraviolet laser, and a system for synchronizing the laser pulses with the phase of the accelerating microwave field. The design parameters of the components of the complex are presented, and the state of research related to its realization is discussed.

1. INTRODUCTION

At present, the photoinjector complexes are actively studied and developed and dozens of such facilities have been created and successfully operated. This interest is primarily related to solving the problems of particle acceleration to high energies and their use as parts of the drivers in the free-electron lasers, which operate in ranges varying from terahertz to X-ray frequencies, as well as to other numerous fundamental applications including superfast electron diffraction and microscopy, etc. Since the time of the first experimental demonstration of photoinjectors [1] significant progress has been reported with respect to almost all their parameters, namely, particle energy, current, brightness, and the repetition rate of electron bunches. In modern microwave photoinjectors [2–5], powerful laser pulses ensure photoemission of the electron bunches from the photocathode with a charge of up to hundreds of nanocoulombs and a duration ranging from femtoseconds to tens of picoseconds. In the case of the appropriate synchronization of a laser pulse and the microwave power-supply source, the electrons emitted from the photocathode are accelerated in the microwave field of the cavity. During the transit through the cavity, they can gain an energy of up to several megaelectron-volts (the obtained electron bunches can be further accelerated up to higher energies). The study of the photoinjector complexes has been actively continued toward creating more perfect new schemes in order to obtain higher peak and average of currents and lower values of the bunch emittance and the particle-energy spread.

The photoinjector complex, which is developed at the Institute of Applied Physics of the Russian Academy of Sciences, has a classical configuration and consists of several subsystems, namely, (i) the accelerating cavity resonator powered by the microwave radiation from a high-stability oscillator, which is

* alvikharev@appl.sci-nnov.ru

Institute of Applied Physics of the Russian Academy of Sciences, Nizhny Novgorod, Russia. Translated from Izvestiya Vysshikh Uchebnykh Zavedenii, Radiofizika, Vol. 63, Nos. 5–6, pp. 477–487, May–June 2020. Original article submitted June 28, 2020; accepted July 30, 2020.

amplified to the multimegawatt power level and ensures the formation of an intense electron bunch, (ii) the photocathode, which is located directly in the cavity and ensures effective emission of electrons, (iii) the ultraviolet laser, which causes photoemission of electrons from the cathode, and (iv) the system of synchronization of the laser pulse with the phase of the accelerating field of the microwave radiation. In this work, the design parameters of the complex components are given and the state of the studies related to the complex realization are discussed.

2. RESONATOR SECTION OF THE MICROWAVE ACCELERATION OF BUNCHES

The small-size amplifier klystron KIU-111 manufactured by the company "Toriy" [6] with a frequency of 2.45 GHz, an output power of 5 MW for the efficiency 44%, a pulse duration of 7 μs, and a gain of up to 50 dB is proposed for use as the microwave-radiation source for the accelerating cavity resonator. The cavity consists of two connected cells such that the lengths of the first and the second cells amount to a quarter and a half of the wavelength, respectively. (Figs. 1*a* and 1*b*). The cavity was calculated and simulated using original software and the three-dimensional commercial code HFSS [7, 8]. According to the developed scheme, the klystron radiation is transported by the waveguide channel on the basis of the standard rectangular waveguides and introduced to the coaxial waveguide at the TEM wave (see Fig. 1*c*), which feeds the accelerating cavity with a length of 117.4 mm. The so-called π mode whose Q-factor amounts to about 13500 according to the simulation is chosen as the operation mode. The frequency of the nearest 0-mode is shifted from the operation-mode frequency by more than 100 MHz. At the operation frequency, the calculated reflection from the resonator section does not exceed -35 dB.

The results of simulating the bunch-formation process in the accelerating cavity are given in Fig. 2. According to this figure, for the accelerating field 70 MW/m and the laser-pulse injection phase about 40° with respect to the microwave-field maximum at the photoinjector output, is expected to have electron bunches with a particle energy of about 3.5 MeV, an emittance of 1.4 mm $\cdot$ mrad, and energy spread not exceeding 0.2%. The bunch charge can reach 100 pC when using the diamond photocathode and about 0.1 pC from a copper photocathode, which is planned to be used in the initial experiments on testing the complex operation.

The electron-energy spread in a bunch is determined by several fundamental factors. First, the electrons emitted from the cathode inevitably have the thermal energy spread and the spread which is determined by the cathode-surface roughness. In the case of a warm copper cathode, both factors amount to about 10–15 eV. Second, despite the fact that the bunch duration is small compared with the period of the high-frequency field, the bunch particles emitted from the cathode surface are injected in slightly different phases of the accelerating field and, therefore, are differently accelerated. To reduce the influence of this factor, the injection phase of the bunch middle was optimized to correspond to the maximum of the energy gained by one electron. In this case, the bunch duration should be reduced (preserving its charge) until the energy spread as a result of the Coulomb repulsion exceeds the spread because of the injection-phase difference. In the case considered, the trade-off value 10 ps was chosen for the bunch duration. Third, the Coulomb repulsion of electrons prevents us from obtaining a monoenergetic bunch. In our case, this factor is considered to be the main one when the bunch charge is about 100 pC.

The scheme which illustrates the vector distribution of the electric field of the operation mode is shown in Fig. 1*a*. Obviously, this distribution on a part of the cathode surface, which is irradiated by the laser, is close to uniform, which is a necessary condition for obtaining the minimum emittance of the bunch. In the case of injection from the cathode, the low-energy electron bunch starts to expand under the action of its natural Coulomb fields so that the emittance increases, as is shown in Fig. 2*b*. As the energy in the accelerating-mode field is increased, the electrons are focused by the magnetic field of the solenoid, which gradually increases from zero at the cathode to the maximum at the accelerating-cavity output. The focusing by the magnetic field prevents the electrons from transverse scatter so that the bunch emittance decreases after reaching some maximum (see Fig. 2*b*). This process can be described in terms of compensation for the correlated angular spread of the particles [9].

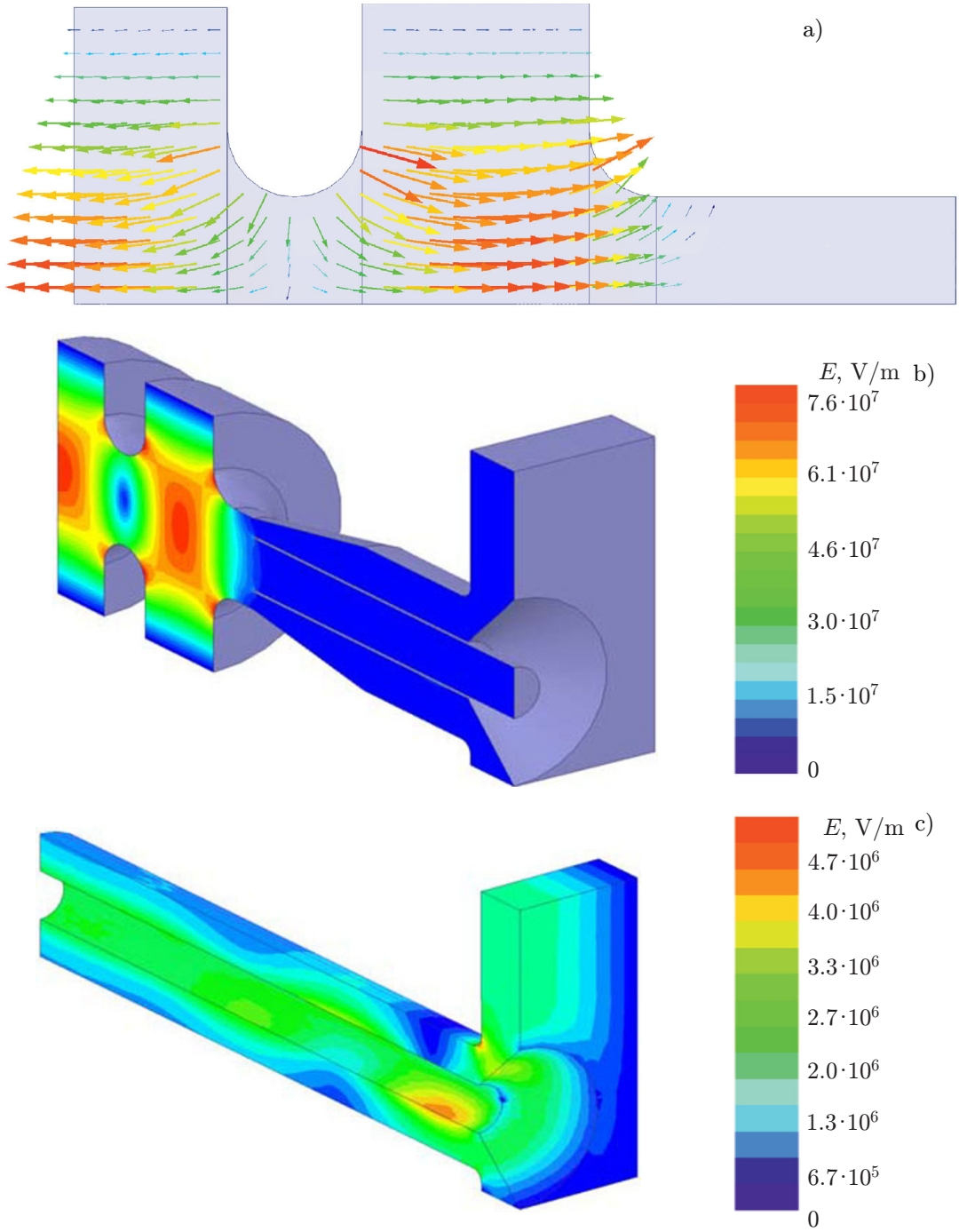

Fig. 1. The scheme of the cavity on the basis of two accelerating cells and the structure of the field of its operation π mode (a) along with the results of the three-dimensional HFSS simulation of the field structures in the accelerating cells (*b*) and the coaxial power input (*c*).

Since the phase of the output signal of the klystron whose stability determines the accelerating-cavity pumping can fluctuate with varying power voltage at the cathode, the requirements for the voltage stability emerge. The simulation shows that the nonuniformity of the voltage pulse of the klystron feed should not exceed 5% for effective pumping of the microwave cavity of the photoinjector with specified Q-factor. In this case, one should have a voltage segment with a duration of at least 2 μs in which a variation in the voltage value does not exceed 1% if the parameter stability with respect to time is no worse than 1% from one pulse to another. The voltage modulator of the KIU-111 55 kV / 250 A / 7 μs / 10 Hz klystron, which meets

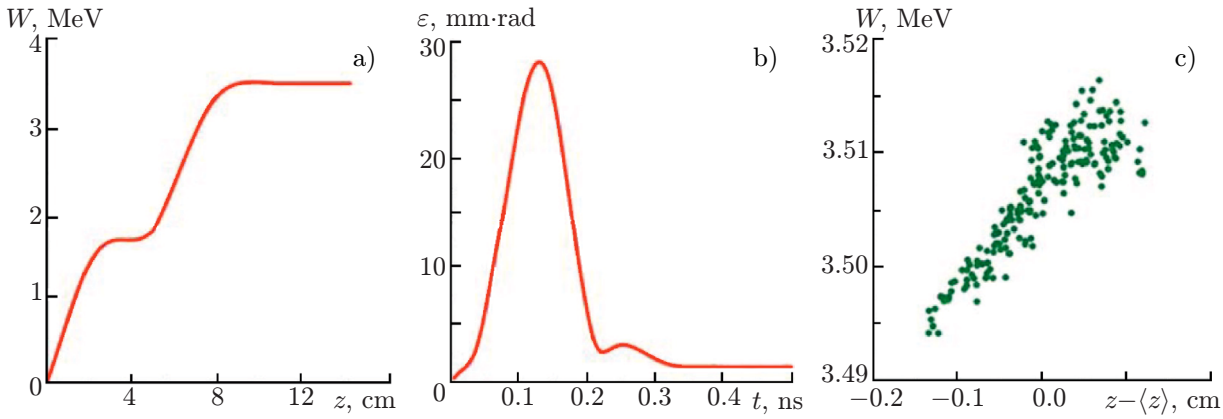

Fig. 2. The results of the microwave-gun simulation: the dependence of the average energy of the particles in a bunch on the cavity length (*a*), evolution of the normalized emittance of the bunch (*b*), and the particle energy distribution in a bunch at the gun output (*c*).

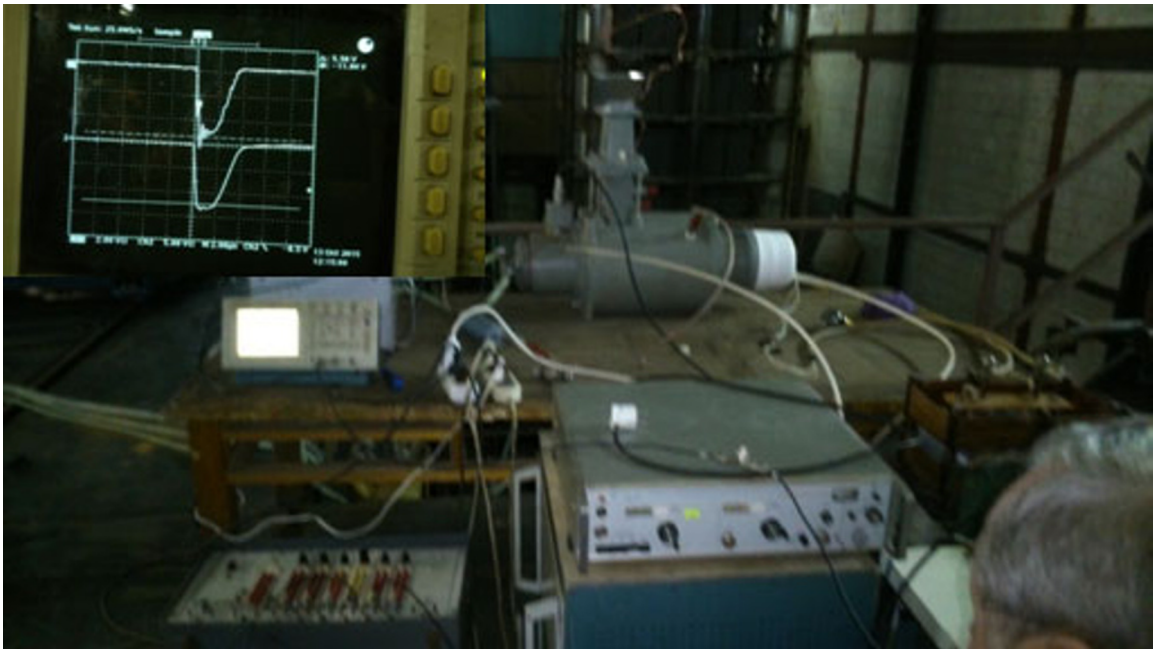

Fig. 3. The results of the experiments on checking the KIU-111-klystron serviceability. The oscilloscope shows the oscillograms of the voltage and microwave-radiation pulses.

these requirements, have been developed and manufactured on the basis of the performed calculations. For comparison, let us note that in this case, the network power of the klystron feed (with allowance for the cathode heater circuit) amounts to about 2 kW, while the power of the feeding system of the laser complex, which is operated with the repetition rate 100 Hz, is about 4 kW. At present, the klystron operation is tested in the model regime in the absence of a load for the output-power level 1 kW (see Fig. 3).

A transmission line has been developed for transporting the microwave radiation from the klystron to the cavity. This line consists of a segment filled with nitrogen under the excess pressure about 1 atm (which is required for the klystron-window operation), a segment with the vacuum pumping, which is separated from the remaining volume of the line by the barrier window on the basis of a thick quartz disk, and the couplers of the direct and reflected signals for the diagnostics of the klystron and cavity operation The gas-inlet section and the pump-out section based on the waveguide with the perforated wall are at the manufacture-completion stage. An important element of the line is the ferrite isolator for 350 W and

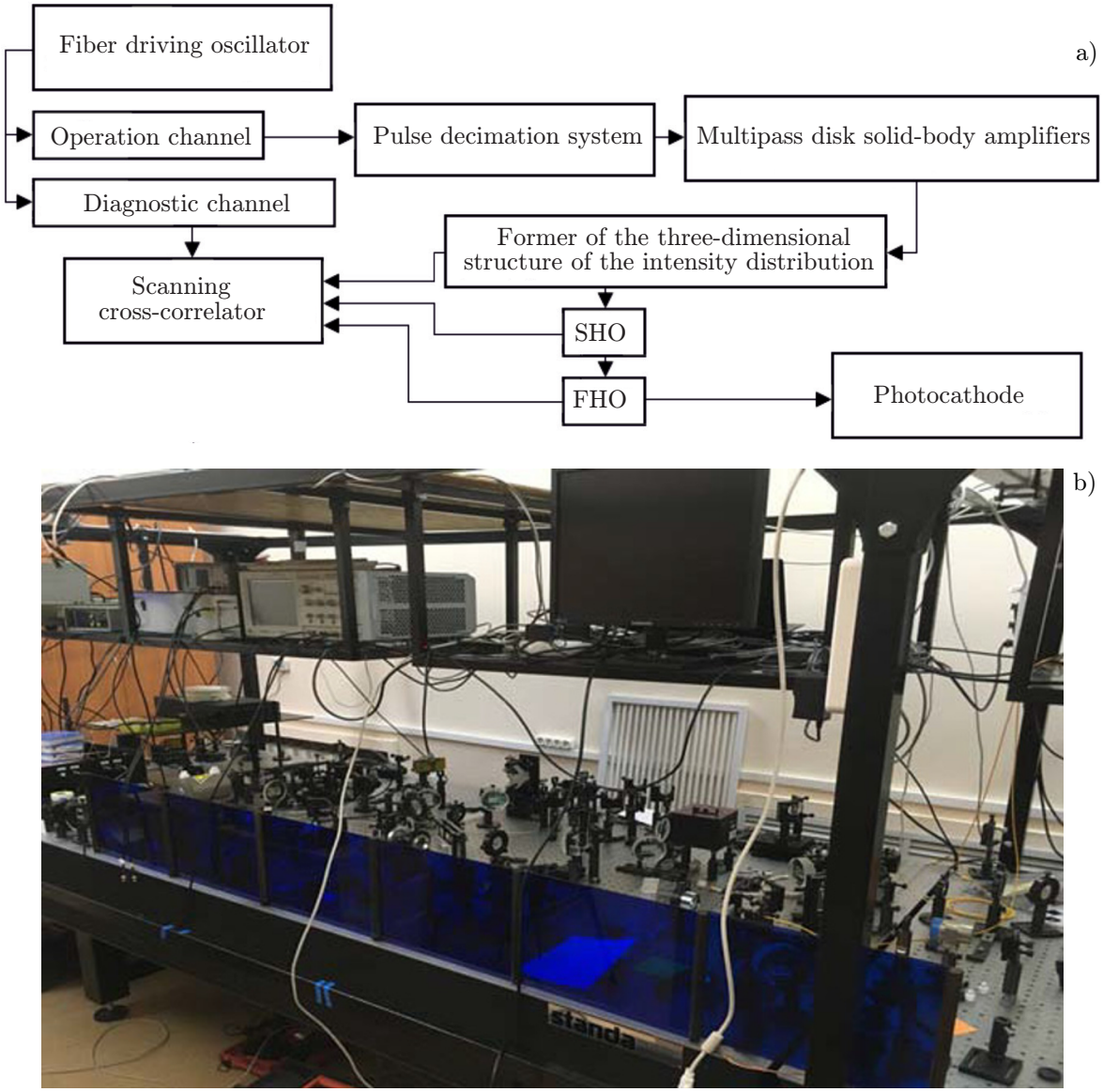

Fig. 4. The diagram (*a*) and the photograph (*b*) of the laser complex for the photocathode irradiation. Here, the SHO and the FHO are used to denote the second- and the fourth-harmonic oscillators, respectively.

5MW of continuous and peak power, respectively, with insulation −20 dB, which should ensure the klystron operation in the presence of reflection from the photoinjector cavity at the beginning of the feeding pulse, as well as during the emergency regimes, e.g., in the case of a breakdown in the accelerating cavity. At present, the assembly of the accelerating cavity and the transmission line is at the completion stage, the cold testing of the complex has started, and the klystron operation at a high (multimegawatt) power level is adjusted.

3. LASER COMPLEX OF THE BUNCH FORMATION

The laser complex with a possibility to control the spectral-time parameters of the laser pulses [10–12], which is created at the Institute of Applied Physics of the Russian Academy of Sciences, will be used for the cathode irradiation. The laser system consists of the starting fiber part, three solid-state amplifies, the formers of the one- and three-dimensional structures of the intensity distribution, the stages for generation of the second and the fourth harmonics, and the system for diagnostics of the laser pulses of the infrared, visible, and ultraviolet bands. The laser diagram is shown in Fig. 4.

The starting part has two output channels (operation and diagnostic) and comprises the fiber driving oscillator (with a pulse repetition rate of 47.6 MHz, a pulse duration amounting to about 250 fs, and a center wavelength of 1034 nm), the optical stretcher on the basis of a chirped fiber Bragg grating, the system of preliminary pulse decimation and the train formation, and the line of the fiber amplifiers with the active fiber doped by Yb^{+3} ions and having a diameter ranging from 7 to 14 μm.

The spectral-phase former, which can also be used for the spectral-amplitude control, is built in the work channel of the fiber part of the laser to control the time form of the laser pulses [10]. The fiber radiation is output outside and collimated, then it travels across the former, returns strictly backwards, and travels through the fiber circulator (the Faraday decoupler) back to the fiber to be additionally amplified in the latter. The former is an optical compressor with zero frequency dispersion in the operation band whose Fourier plane has a Hamamatsu spatial light modulator (SLM). company.

Using the former, one can control the form of the spectral distribution of intensity of the broadband linearly chirped laser pulses (spectrons). For them, the spectrum-intensity distribution corresponds to the intensity distribution in time, i.e., the spectrum control allows us to directly control the time form of the pulse. Using the former, the laser pulses with a rectangular [10] and linearly increasing (triangular) intensity distribution in time [12] have already been obtained in the infrared region of the spectrum. At the output of the fiber part of the laser, the duration of the pulses of the operation and diagnostic channels amounts to about 200 ps. Using the optical compressor, the diagnostic-channel pulses are compressed to their Fourier limit 250 fs and directed to the scanning cross-correlator, in which they are used for the diagnostics of the three-dimensional shape of the profiled pulses of the infrared, visible, and ultraviolet bands (see Fig. 4).

The radiation from the fiber output of the operation channel is directed to an additional decimation system, which was created on the basis of the Pockels cell. This system allows one to form the final train of pulses (or a single pulse if required) for the subsequent amplification, transformation into the ultraviolet range, and generation of the electron bunches from the surface of the cathode of the electron photoinjector. Three multipass disk amplifiers with a diode pumping of 300 W/1 kW and a central wavelength of 940 nm are used to increase the laser-pulse energy. The 3 mm-thick Yb:KGW crystals were used as active elements. The stage of formation of a three-dimensional structure of laser pulses, which consists of an optical compressor to control the duration in the range 0.25–200 ps and the volume chirped Bragg grating, which can be used for creating the laser pulses with the three-dimensional ellipsoidal intensity distribution [10], is located after the amplifiers. The stage of generation of the second and the fourth harmonics, at which it is supposed to transform the radiation from the infrared to the ultraviolet range of the spectrum, is located next and followed by the lens transmission line to direct the ultraviolet radiation to the cathode surface.

4. SYNCHRONIZATION SYSTEM

To feed the klystron, use is made of the two-step system of a low-power microwave source and a preamplifier (Fig. 5), which ensures an output power of up to 200 W for continuous input power 0.5–3 mW in the case of the pulse duration up to 7 μs and the repetition rate up to 100 Hz.

The klystron operation range is rather narrow, namely, 2445 ± 5 MHz. The radiation frequency of the stabilized microwave source should fall within this range and remain stable for a long time. A module ZX95-2490-S manufactured by Mini Circuits, which is operated in the range 2290–2490 MHz with an output-signal power of + 8 dBm, is used as such a source, i.e., a voltage-controlled oscillator (VCO). The voltage-controlled oscillator allows us to use the phase-locked loop (PLL) for the reference frequency of any source with good spectral characteristics so that the reference frequency can differ ten-fold from the specified frequency. The PLLs are successfully used for synchronizing the microwave sources, which operate at frequencies of up to hundreds of gigahertz and are used in the systems of precision laboratory spectroscopic measurements [13].

The frequency is stabilized by the PLL on the basis of the PE3336 microcircuit manufactured by Peregrine Semiconductor with the maximum input frequency 3 GHz. The microcircuit contains the required frequency dividers in the signal and reference-frequency channels, as well as the internal frequency-phase detector (FPD) with the maximum frequency 20 MHz of the input signals and the system of indicating the

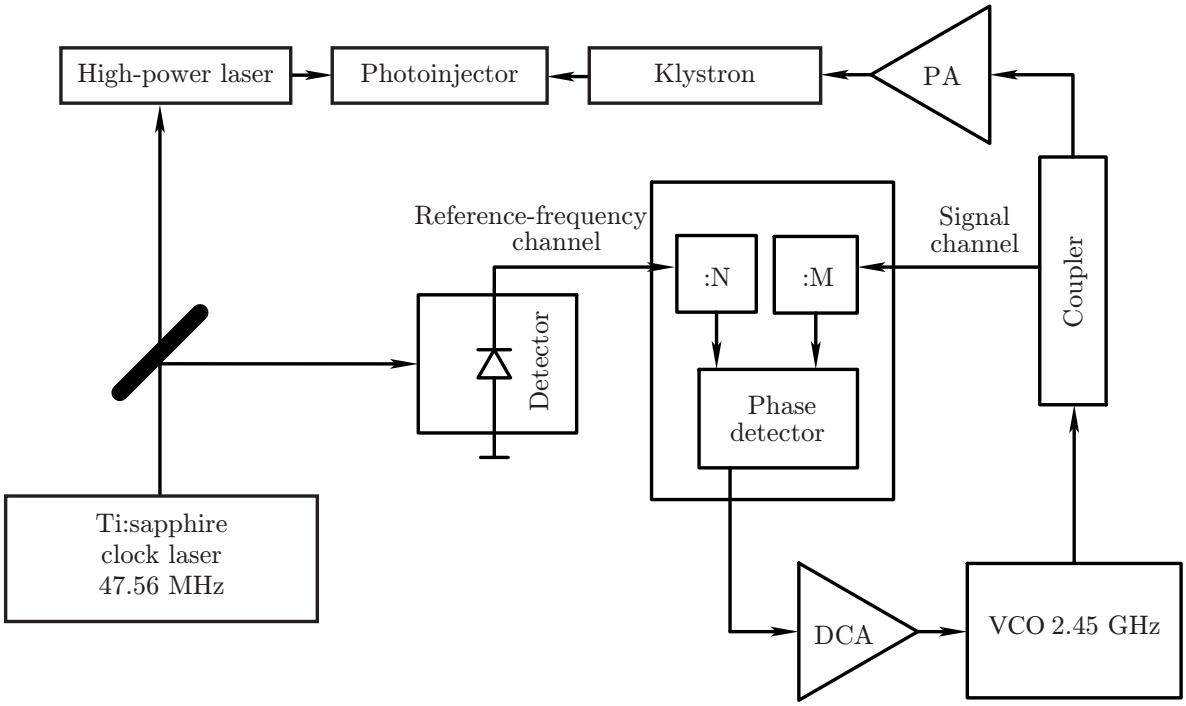

Fig. 5. The circuit diagram of the system of synchronization of the laser pulses and the accelerating microwave pulses (here, the DCA and the PA are used to denote the direct-current amplifier and the power amplifier, respectively).

synchronization regime (a similar element was successfully used in a radiometric ozonometer [14]).

The reference signal is formed from the pulse train, which is generated by the photoreceiver under the action of the femtosecond-laser radiation branched to the photoreceiver. Under the action of the laser pulses, the photoreceiver generates short (no longer than tens of nanoseconds) current pulses with the repetition rate of the laser-radiation pulses and then these pulses are transformed to pulses with halved frequency and a duty ratio of about 50% (i.e., meander), which can be used for operation of digital logic microcircuits. After the required amplification, the filtered main harmonic of this signal is supplied to the full-wave frequency doubler. As a result of filtering and amplification of the main harmonic of the signal, we obtain a sinusoidal signal whose level is independent of variation in the laser-pulse repetition rate and the parameters of the circuits forming these pulses. Such a signal is to a lesser degree subject to the phase jitter, which can deteriorate the phase stability of the signal of the synchronized microwave source. The exact tuning to the required frequency in the operation band of the microwave power amplifier, which is used for the klystron feeding, is performed by choosing the frequency dividers in the channel of the signal (which is taken from the directional coupler at the VCO output) and the reference frequency obtained from the repetition rate of the femtosecond laser. The successful operation of the microwave source for the laboratory measurements, which is stabilized by the reference signal of the femtosecond laser, is shown in [15].

To ensure exact tuning of synchronization of the laser and microwave radiation, the reference signal of the PLL is adjusted by the phase shifter whose design is similar to that of the phase modulator in [16]. To ensure constant phase shift of the signal, direct voltage, which is proportional to the phase shift, is supplied to the second input of the comparator instead of the modulating alternating voltage.

5. PHOTOCATHODES ON THE BASIS OF THE DIAMOND FILMS

Diamond is considered to be one of the promising materials for the photocathodes, which form electron bunches for modern accelerators including those based on photoinjectors. Diamond has some unique properties, such as radiation strength, the high charge-carrier mobility and thermal conductivity, and

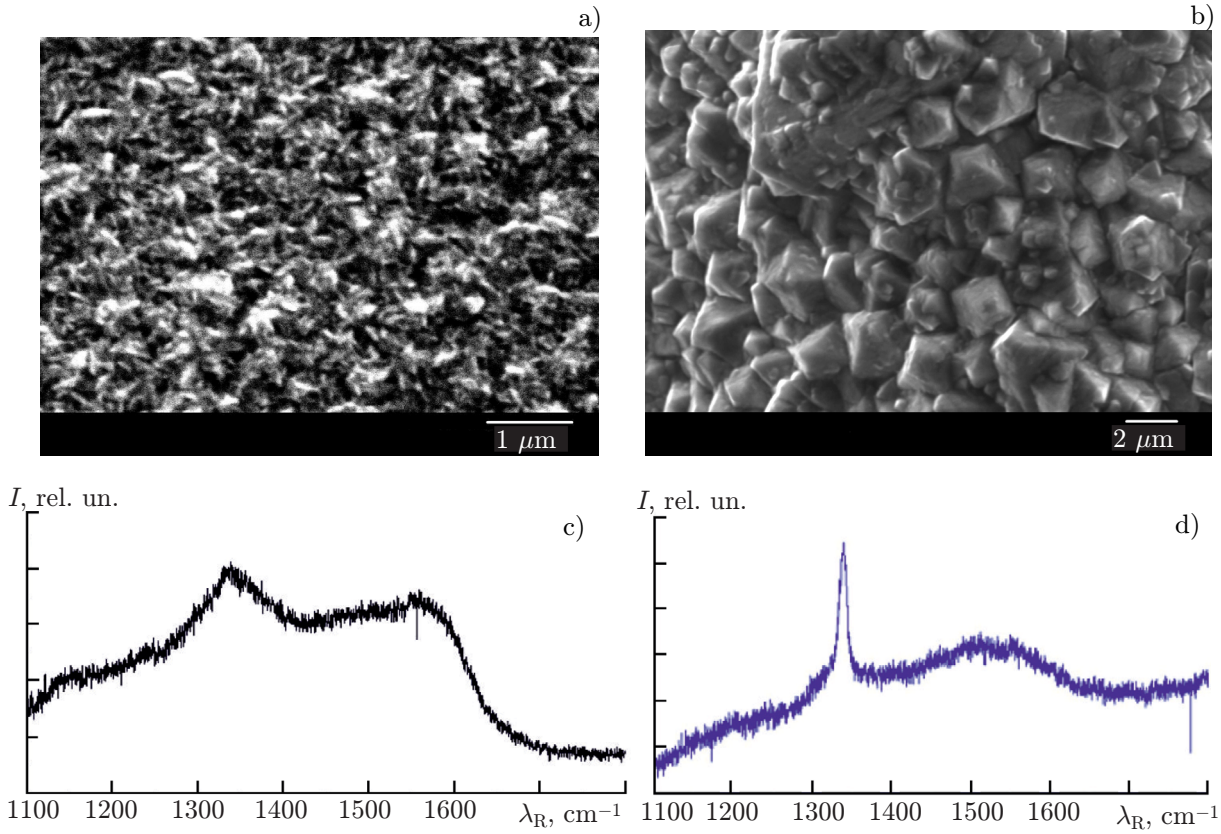

Fig. 6. Microphotographs of the surface (top) and the Raman spectrum λ_{R} (bottom) of the diamond film after the first (*a* and *c*) and the second (*b* and *d*) stages of deposition onto the molybdenum substrate.

a possibility of reaching negative electron affinity, and, therefore, the work-function reduction. Moreover, the diamond photocathode is not critical to the vacuum level, is easily cleaned, and recovers the emission properties even after being exposed to air.

In the developed photoinjector complex, it is assumed to use the diamond photocathode consisting of several layers of a nanocrystalline diamond film with a thickness of 0.1 to 2 μm, which is deposited from the gas phase in a microwave plasma-chemical reactor. The first, photoabsorbing layer is a diamond with the n-type conduction, which is strongly doped by nitrogen or phosphorus. Doping makes it possible to produce photoelectrons using cheaper long-wavelength lasers (with wavelength exceeding 200 nm) of the optical range, which ensure photoionization from the donor levels with activation energies of 1.6 eV and 0.6 eV for nitrogen and phosphorus, respectively. According to the estimates, for the nitrogen-admixture number density $10^{20}\,\mathrm{cm}^{-3}$, the absorption length of the laser radiation with a wavelength of 532 nm lies in the range 0.1–1 μm [17] and the charge resulting from the photoabsorption can reach 100 pC. In this case, the presence of conduction of the diamond film impedes the charge accumulation on the photocathode surface, which ensures the photoinjector operation for a high repetition rate of the laser pulses. The second layer, which is the weakly doped diamond, is required to provide the electron and hole drift to the emitting surface of the diamond during which the electron thermalization, which reduces the energy spread and emittance of the electron beam, occurs because of the collisional mechanism. The third layer is the H-terminated layer with a low or negative work function. In this case, the presence of the second and the third layers of the weakly-doped nanocrystalline film with conduction and high transparence in the ultraviolet and visible parts of the spectrum [18] do not impede the transport of the ionizing laser radiation from the side of these layers to the absorbing layer.

On the whole, such a cathode has a great quantum efficiency and the required electrical-conductivity level [19]. In the case of ultraviolet irradiation of the diamond film, these properties allow a great number

of electrons to be efficiently emitted from the surface and new electrons to be supplied to it. In particular, a quantum efficiency of about 10^{-3} for the nitrogen-doped nanocrystalline diamond film with the hydrogen-passivated surface [20] was experimentally obtained in the case of irradiation with a wavelength of 254 nm. The above-mentioned quantum efficiency significantly exceeds the well-known quantum efficiency for monocrystalline copper ($5 \cdot 10^{-5}$), which is sometimes used as a material for the photocathode in acceleration applications. At present, deposition of multilayered nanocrystalline diamond films with various degrees of doping (with the impurity content 10^{18}–10^{21} cm^{-3}) by both nitrogen and phosphorous (n type) and boron (p type) onto the metal-substrate surface has been studied. Figure 6 shows the microphotographs (obtained using the scanning election microscope) of the surface of the first nitrogen-doped layer and the second undoped layer, which were successively deposited onto the molybdenum substrate, and their Raman spectra. The spectrum of the nitrogen-doped film (Fig. 6*c*) has two wide peaks in the vicinities of 1350 cm^{-1} and 1580 cm^{-1}, which is indicative of the fact that it contains nanocrystalline diamond and sp^2-hybridized carbon [21]. The high quality of the undoped film is confirmed by a high peak near 1332 cm^{-1}, which is typical of the diamond sp^3 phase of carbon, and a weak band in the vicinity of 1550 cm^{-1}, which is related to the presence of the sp^2 phase (see Fig. 6*d*). As a result, the photocathode surface is a two-layered structure consisting of a photon-absorbing nanocrystalline film, which is strongly doped by nitrogen and has a high conductivity, and a thin diamond film which is applied on top of the above-described film.

Therefore, the studies have shown that the morphology of the films, their conductivity, and the content of the fraction of the non-diamond phase in these films considerably depend on the deposition regime, which, in turn, significantly influences their emission properties. In the following stage, it is assumed to test the photocathode on the basis of the nanocrystalline diamond films in the developed photoinjector complex.

The photoinjector development (Secs. 2–4) was partially supported by the Russian Science Foundation (project No. 20–12–00378). The deposition and characteristics of the nanocrystalline diamond films (Sec. 5) were studied within the framework of the state assignment to the Institute of Applied Physics of the Russian Academy of Sciences (project No. 0035–2019–0003).

REFERENCES

1. J. S. Fraser, R. L. Sheffield, E. R. Gray, and G. W. Rodenz, *IEEE Trans. Nucl. Sci.*, **32**, No. 5, 1791–1793 (1985). https://doi.org/10.1109/TNS.1985.4333725
2. J. B. Rosenzweig, N. Barov, and E. Colby, *IEEE Trans. Plasma Sci.*, **24**, No. 2, 409–420 (1996). https://doi.org/10.1109/27.510005
3. R. Akre, D. Dowell, P. Emma, et al., *Phys. Rev. ST Accel. Beams*, **11**, No. 3, 030703 (2008). https://doi.org/10.1103/PhysRevSTAB.11.030703
4. F. Stephan, C. H. Boulware, M. Krasilnikov, et al., *Phys. Rev. ST Accel. Beams*, **13**, No. 2, 020704 (2010). https://doi.org/10.1103/PhysRevSTAB.13.020704
5. J. G. Power, in: *AIP Conf. Proc.*, **1299**, 20–28 (2010). https://doi.org/10.1063/1.3520316
6. http://www.toriy.ru/ru/kly.html
7. S. V. Kuzikov, S. Shchelkunov, and A. A. Vikharev, in: *AIP Conf. Proc.*, **1812**, 080005 (2017). https://doi.org/10.1063/1.4975891
8. S. V. Kuzikov, S. A. Bogdanov, E. I. Gacheva, et al., in: *Proc. 38th Int. Free-Electron Laser Conf. (FEL-2017), August 20–25, 2017, Santa Fe, USA*, pp. 436–438. https://doi.org/10.18429/JACoW-FEL2017-WEP012
9. L. Serafini and J. Rosenzweig, *Phys. Rev. E*, **55**, No. 6, 7565–7590 (1997). https://doi.org/10.1103/PhysRevE.55.7565

10. S. Y. Mironov, A. K. Poteomkin, E. I. Gacheva, et al., *Laser Phys. Lett.*, **13**, No. 5, 055003 (2016). https://doi.org/10.1088/1612-2011/13/5/055003
11. S. Yu. Mironov, A. V. Andrianov, E. I. Gacheva, et al., *Phys. Usp.*, **60**, No. 10, 1039–1050 (2017). https://doi.org/10.3367/UFNe.2017.03.038143
12. I. Kuzmin, S. Mironov, E. Gacheva, et al., *Laser Phys. Lett.*, **16**, No. 1, 015001 (2019). https://doi.org/10.1088/1612-202X/aaef95
13. Yu. I. Alekshin, G. M. Altshuller, O. N. Pavlovsky, et al., *Int. J. Infrared Millim. Waves*, **11**, No. 8, 961–971 (1990). https://doi.org/10.1007/BF01008638
14. A. A. Krasil'nikov, Yu. Yu. Kulikov, V. G. Ryskin, et al., *Instrum. Exp. Tech.*, **54**, No. 1, 118–123 (2011). https://doi.org/10.1134/S0020441211010167
15. D. S. Makarov, M. Yu. Tretyakov, A. P. Shkaev, et al., *Appl. Phys. Lett.*, **105**, No. 6, 063502 (2014). https://doi.org/10.1063/1.4891503
16. J. Doose, A. Guarnieri, W. Neustock, et al., *Z. Naturforsch.*, **44**, No. 6, 538–550 (1989). https://doi.org/10.1515/zna-1989-0609
17. R. P. Mildren and J. Rabeau, eds., *Optical Engineering of Diamond*, Wiley–VCH, Weinheim,(2013).
18. N. A. Feoktistov, S. A. Grudinkin, M. V. Rybin, et al., *Tech. Phys. Lett.*, **37**, No. 4, 322–325 (2011). https://doi.org/10.1134/S1063785011040079
19. A. L. Vikharev, O. A. Ivanov, and S. V. Kuzikov, "Diamond photocathode" [in Russian], RF Patent No. 2658580 (2018).
20. K. J. P. Quintero, S. Antipov, A. V. Sumant, et al., *Appl. Phys. Lett.*, **105**, No. 12, 123103 (2014). https://doi.org/10.1063/1.4896418
21. O. A. Williams, *Diam. Rel. Mater.*, **20**, Nos. 5–6, 621–640 (2011). https://doi.org/10.1016/j.diamond.2011.02.015